Applied Environmental Research
- RESEARCH FOR SUSTAINABLE PLANET -

Research Article

Application of Fe_3O_4/thiamine Magnetic Particles in the Removal of Methylene Blue

Phuong Lan Tran-Nguyen[1,*], Suong Mai-Thi-Thu[2], Thanh-Ty Nguyen[2], Kim-Phung Ly[2], Luu-Ngoc-Hanh Cao[2], Tran Thi Bich Quyen[2], Shella Permatasari Santoso[3], Nguyen-Phuong-Dung Tran[4], Nguyen Minh Nhut[2,]**

[1] *Faculty of Mechanical Engineering, Can Tho University, Can Tho City 900100, Vietnam*
[2] *Faculty of Chemical Engineering, Can Tho University, Can Tho City 900100, Vietnam*
[3] *Department of Chemical Engineering, Widya Mandala Surabaya Catholic University, Surabaya 60133, Indonesia*
[4] *Department of Material Science and Engineering, National Taiwan University of Science and Technology, Taipei, 106, Taiwan*

[*,**]Correspondence Email: tnplan@ctu.edu.vn; nmnhut@ctu.edu.vn

Abstract

Fe_3O_4/thiamine particles were prepared in this work via precipitation method. The synthesis method is based on the principle of precipitation of Fe_3O_4 particles in the presence of thiamine coating agent. Also, the potential application of Fe_3O_4/thiamine in the removal of methylene blue (MB) was investigated. Several factors that affect the synthesis of Fe_3O_4/thiamine such as base concentration, mass ratio of $FeCl_2$ to thiamine, reaction temperature, and reaction time were determined. Optimal conditions for preparing Fe_3O_4/thiamine are NH_4OH concentration = 10%, mass ratio of $FeCl_2$:thiamine = 5:1 (g g^{-1}), reaction temperature = 30 °C, reaction time = 120 min. The average particle size of Fe_3O_4/thiamine is 293.7 nm while the specific surface area, pore diameter, and magnetization of the obtained Fe_3O_4/ thiamine particles are 57 m^2 g^{-1}, 192.67 Å, and 2.4 emu g^{-1}, respectively. The interesting point of this work is to obtain the Fe_3O_4/thiamine at low temperature with less amount of NH_4OH used. Furthermore, 79.08% of MB could be removed using Fe_3O_4/thiamine as an adsorbent, with a maximum adsorption capacity of 31.63 mg g^{-1} at pH of 10, a MB concentration of 50 mg L^{-1}, and an adsorption time of 15 min. Adsorption kinetics studies showed that the pseudo-second-order model fitted the experimental data better than the pseudo-first-order and the adsorption process is physical adsorption following the Freundlich adsorption isotherm model. An adsorption mechanism of MB onto Fe_3O_4/thiamine was also suggested. The synthesized Fe_3O_4/ thiamine particles could be a potential material for treating wastewater.

ARTICLE HISTORY

Received: 12 Dec. 2022
Accepted: 9 Jul. 2023
Published: 6 Oct. 2023

KEYWORDS

Adsorption;
Fe_3O_4/thiamine;
Methylene blue;
Precipitation method

Introduction

Most synthetic dyes are toxic, mutagenic, carcinogenic, cause environmental pollutants, and difficult to decompose [1]. Wastes from untreated organic dyes will hurt plants, aquatic life, and humans. Methylene blue (MB) is a hazardous cationic dye, which harms human health such as increased heart rate, vomiting, shock, cyanosis, jaundice and quadriplegia, and tissue necrosis [2]. Thus, the selection of a suitable method for MB removal from water effluent is important. Among the methods for treating waste water, adsorption gets the attention from scientists and is widely used for the treatment of organic and inorganic pollutants [3–5]. Adsorption can be advantageous over other methods due to that it is a simple process as well as low cost [6–7].

In recent years, nano-magnetic materials have attracted the interest of researchers because of their high stability, high magnetic, easy to synthesize and reuse, and low cost [7–8]. Fe_3O_4 can be synthesized by different methods such as sol-gel, thermal decomposition, co-precipitation, micro-emulsion, and precipitation [9–13]. Some studies evaluating MB adsorption capacity by magnetic materials were conducted such as Fe_3O_4, CTS@SnO_2@Fe_3O_4, Fe_3O_4@MIL-100 (Fe) [14–16]. The oxidation of Fe_3O_4

https://doi.org/10.35762/AER.2023018

easily occurred during storage conditions; thus, materials-coated Fe_3O_4 is necessary. Thiamine, as a biocompatible modifier to prevent the oxidation of Fe_3O_4, is cheap, stable and non-toxic [17].

Thiamine, composed of pyrimidine and thiazole rings joined by a methylene bridge, is a possible growth factor that is required for textile wastewater treatment systems and significant for the removal of dissolved organic carbon, chemical oxygen demand, and oxygen uptake rate [18]. Thiamine may speed up the treatment process of textile dye wastewater and make it treatable. Thiamine is also an important coenzyme for active sludge microorganisms in textile dye wastewater treatment systems [18]. Besides, thiamine-coated materials were also evaluated for the possible removal of Cd(II), phosphate, and divalent copper ions [17, 19– 20].

From a literature review, the reliable results for the MB removal in wastewater using Fe_3O_4/thiamine were implemented by only a few studies. This work investigated the reaction conditions of Fe_3O_4/thiamine formation such as mass ratio of Fe_3O_4 to thiamine, concentration of NH_4OH, reaction time, and reaction temperature. The other objective was to perform simple and effective reaction and evaluated the application of Fe_3O_4/ thiamine on the removal of MB. The main parameters investigated including pH, adsorbent dosage, MB concentration and contact time. Furthermore, several adsorption isotherm models (Langmuir, Freundlich and Dubinin–Radushkevich) and adsorption kinetic models (pseudo-first-order and pseudo-second-order) were fitted to find out the adsorption mechanism of MB onto Fe_3O_4/ thiamine.

Materials and methods

1) Chemicals

Iron(II) chloride tetrahydrate ($FeCl_2{\cdot}4H_2O$, 98%), ammonium hydroxide solution (NH_4OH, 25–28%), methylene blue ($C_{16}H_{18}ClN_3S$, 85%), hydrochloric acid (HCl, 36–38%), potassium hydroxide (KOH, 90%), potassium chloride (KCl, 99%), ethanol (C_2H_5OH, 96%), and thiamine ($C_{11}H_{16}ClN_4OS$, 99%) were purchased from Merck (Germany). All chemicals were analytical grades and directly used without purification.

2) Synthesis of Fe_3O_4/thiamine

The synthesis of Fe_3O_4/thiamine is based on the methods of Tran-Nguyen et al. [20] and Shaterian and Molaei [21] with some modifications and is depicted in Figure 1. Firstly, 50 mL of $FeCl_2$ solution was mixed with 50 mL of thiamine solution with a mass ratio 1:1 – 10:1 in a two-necked flask. The mixture was stirred at 500 rpm and heated to the desired temperature T (30 – 90 °C). The reflux system was installed to prevent the evaporation of solution during reaction. After reaching the desired temperature, 30 mL of NH_4OH solution with the desired concentration (10 – 25%) was added dropwise to the mixture and kept at temperature T (°C) for a desired time t (30 – 120 min). After the reaction, black particles from the suspension were separated by a magnet and washed several times with distilled water and 96% ethanol till neutral pH. The product was dried at 60 °C until constant weight and stored in a desiccator before conducting further experiments. For each of the configurations, three separate experiments were performed to analyze the uncertainty.

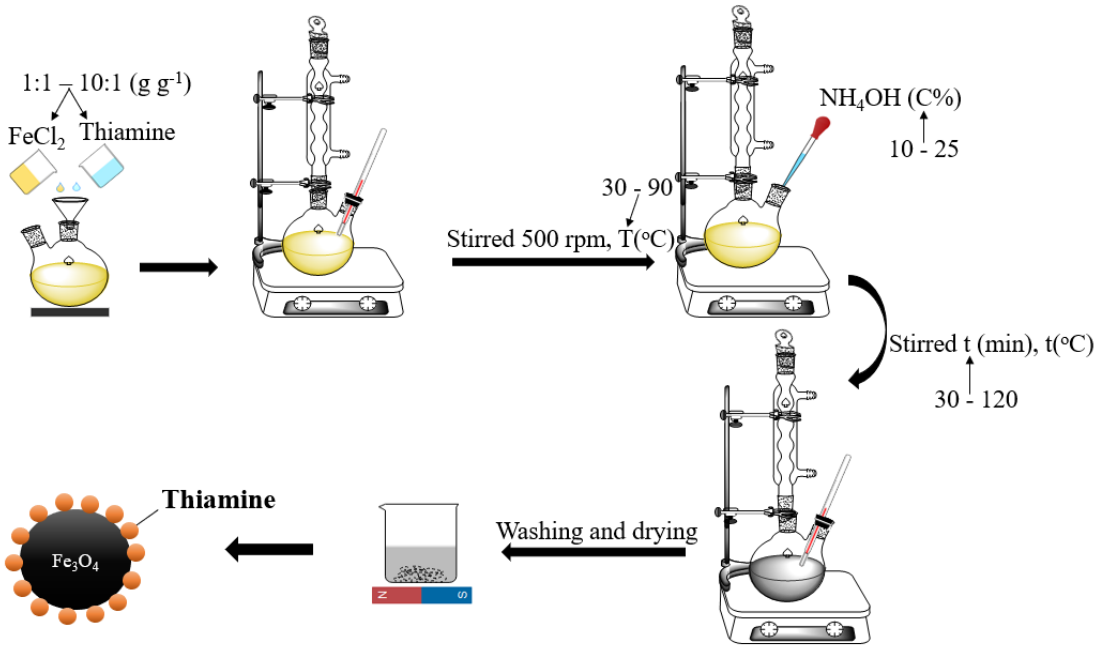

Figure 1 The synthesis process of Fe_3O_4/thiamine.

Characterizations

The morphology of Fe_3O_4/thiamine was characterized by Transmission electron microscopy (TEM; TECNAI G2-20). X-ray diffraction (XRD) was applied for determining the crystallographic structure while Fourier transformed infrared spectroscopy (FTIR; Thermo Nicolet 6700) with the scanning range from 4,000 – 400 cm^{-1} allowed the qualitative analysis to detect functional groups and characterize bonding information. Brunauer–Emmett–Teller (BET; Nova 1000e) was applied to determine the specific surface area and pore size. Besides, Dynamic light scattering (DLS; SZ-100Z2) and a vibrating sample magnetometer (VSM; DMS 880) were also applied.

3) Adsorption experiments

The stock solution of MB was prepared by dissolving 1 g of MB in 1 L of deionized water, and then diluted to obtain solutions at lower concentrations. Adsorbent (1.25 to 10 g L^{-1}) was placed in an Erlenmeyer flask. MB solution (20 mL) was, then, added and shaken at 100 rpm. The effects of MB concentration (10 – 60 mg L^{-1}), pH (6 – 11) and adsorption time (30 – 90 min) were investigated at room temperature. After adsorption, the absorbent was magnetically separated from the MB solution. The concentration of MB solution before and after adsorption were measured using a Thermo Scientific Evolution 60S UV-Visible Spectrophotometer at 664 nm to determine the adsorption efficiency and capacity. The adsorption efficiency and the adsorption capacity were calculated as follows:

$$\text{Removal efficiency (\%)} = \frac{C_0 - C_t}{C_0} \times 100 \qquad \text{(Eq. 1)}$$

$$\text{Adsorption capacity (mg. g}^{-1}) = \frac{C_0 - C_t}{m} \times V \qquad \text{(Eq. 2)}$$

where m (g) is the adsorbent weight, V (L) is the volume of MB solution, Co (mg L^{-1}) and Ct (mg L^{-1}) are the initial concentration of MB solution and the concentration of MB solution at time t, respectively. The experimental data were matched with first-pseudo-order and pseudo-second-order kinetic models to understand the mechanism of MB adsorption on Fe_3O_4/thiamine [22] and these mathematical models are presented in Eq. 3 and Eq. 4:

$$\ln (q_e - q_t) = \ln q_e + k_1 t \qquad \text{(Eq. 3)}$$

$$\frac{t}{q_t} = \frac{1}{k_2 q_e^2} + \frac{t}{q_e} \qquad \text{(Eq. 4)}$$

where q_e (mg g^{-1}) and q_t (mg g^{-1}) are the adsorption capacity at equilibrium and the adsorption capacity at time t, respectively; k_1 (min^{-1}) and k^2 (g mg^{-1} min^{-1}) are the rate constants of pseudo-first-order model and pseudo-second-order model, respectively; and t (min) is the contact time. Adsorption isotherm models including Langmuir, Freundlich and Dubinin–Radushkevich were also explored by fitting the experimental data to the models at different MB concentrations (10, 20, 30, 40, 50 and 60 mg L^{-1}) [22–23]. The linear mathematical models (Langmuir, Freundlich and Dubinin-Radushkevich models) are expressed in Eq. 5, Eq. 6 and Eq. 7, respectively:

$$\frac{C_e}{q_e} = \frac{1}{q_{max} k_L} + \frac{C_e}{q_{max}} \qquad \text{(Eq. 5)}$$

$$\ln q_e = \ln k_F + \frac{\ln C_e}{n} \qquad \text{(Eq. 6)}$$

$$\ln q_e = \ln q_D - \beta \varepsilon^2 \qquad \text{(Eq. 7)}$$

where C_e (mg L^{-1}) is the dye concentration at equilibrium; q_e (mg g^{-1}) and q_{max} (mg g^{-1}) are the equilibrium adsorption capacity and the maximum adsorption capacity, respectively; k_L is a characteristic constant of the Langmuir model; k_F is the constant of the Freundlich model, n is the constant indicating adsorption intensity; q_D (mg g^{-1}) is the adsorption capacity based on Dubinin-Radushkevich, β is the constant corresponding to the adsorption energy (mol^2 kJ^{-2}), R is the gas constant (8.314 J mol^{-1} K^{-1}), T is the temperature of process (K), and ε is the Polanyi potential and can be calculated by Eq. 8.

$$\varepsilon = RT \ln\left(1 + \frac{1}{C_e}\right) \qquad \text{(Eq. 8)}$$

4) Desorption

After adsorption, Fe_3O_4/thiamine was tested for the desorption to assess the reusability. The desorption experiments were performed by adding 15 mL 0.1 M HCl into Fe_3O_4/thiamine after adsorption at optimal conditions and shook for 15 min. The desorbed material was separated and used for the next adsorption experiments [24]. An exact amount of desorbed Fe_3O_4/thiamine and 20 mL of MB solution were placed in an Erlenmeyer flask and shaken for a fixed time to examine the reusability of Fe_3O_4/thiamine.

Results and discussion

1) Characterization of Fe_3O_4/thiamine

Alkali is an important factor in the synthesis of magnetic nanoparticles. Compared to KOH and NaOH, the OH- group in NH_4OH is released more slowly, resulting in more uniform and controllable particle sizes [25]. In this work, NH_4OH was used as the alkali for the material synthesis. The presence of NH_4OH solution (%) strongly affects the Fe_3O_4 particles formation which is described as follows:

$$4FeCl_2 + 8NH_4OH + O_2 \rightarrow 4FeOOH + 8NH_4Cl + 2H_2O \quad \text{(Eq. 9)}$$

(orange)

$$FeCl_2 + 2NH_4OH \rightarrow Fe(OH)_2 \downarrow + 8NH_4Cl \quad \text{(Eq. 10)}$$

(blue)

$$FeOOH + Fe(OH)_2 \rightarrow Fe_3O_4 + H_2O \quad \text{(Eq. 11)}$$

$$4Fe_3O_4 + O_2 \rightarrow 6Fe_2O_3 \quad \text{(Eq. 12)}$$

Intermediate products (FeOOH and Fe_2O_3) were formed during the synthesis process while the reaction between FeOOH and $Fe(OH)_2$ could produce Fe_3O_4. The presence of more base resulted in forming more by-products such as FeOOH, Fe_2O_3. The effect of NH_4OH solution concentration was firstly examined. Other factors that were fixed are: mass ratio of $FeCl_2$:thiamine = 1:1 (g g^{-1}), reaction temperature = 90 °C and reaction time = 60 min. Figure 2(a) shows the characteristic peaks of Fe_3O_4 at 2θ = 30.25°, 35°, 43.23°, 55.19°, 57.17°, 62.69°, corresponding to planes (220), (311), (400), (422), (511), and (440), respectively fitting to JCPDS standard card No. 01-072-2303 [26]. Fe_3O_4/thiamine could be formed at the lowest NH_4OH concentration (10%). As this concentration was increased to 15%, both Fe_2O_3 and FeOOH were formed. With higher concentrations of 20% and 25%, the presence of Fe_2O_3 is clearly seen in the final product. The appearance of Fe_2O_3 can be generated during the reaction of partially oxidized magnetite. Besides, FeOOH may appear during the oxidation reaction of Fe_3O_4 and washing steps [26–27]. A faster reaction occurred at a higher base concentration, resulting in more by-products created. Therefore, a concentration of 10% is appropriate for the synthesis of Fe_3O_4/thiamine.

Since magnetic nanoparticles are prone to oxidation, thiamine is considered for reducing the oxidation speed of Fe_3O_4 and increasing the adsorption capacity. The characteristic peaks of Fe_3O_4 at different mass ratios of $FeCl_2.4H_2O$: thiamine (with the base of NH_4OH – 10% at 90 °C within 60 min) and there are no by-products identified in Figure 2(b). The intensity of the diffraction peaks increases with increasing $FeCl_2.4H_2O$: thiamine ratio. The lattice constants corresponding to the ratios of $FeCl_2.4H_2O$: thiamine of 1:1, 3.1, 5.1 and 10.1 are 8.3692 Å, 8.3759 Å, 8.3812 Å, and 8.3801 Å, respectively, which are between the lattice constants of γ-Fe_2O_3 (8.345 Å) and Fe_3O_4 (8.396 Å). The lattice constant value is chosen as the closest to the systematic lattice constant of the Fe_3O_4 phase [27]; thus, the ratio of 5:1 was selected.

As the reaction temperature was changed from 30 to 90 °C at 10% concentration of NH_4OH and $FeCl_2$: thiamine mass ratio of 5:1 (g g^{-1}) during 60 min, the characteristic diffraction peaks for Fe_3O_4 are indicated at 2θ = 30.29°, 35.66°, 43.31°, 53.73°, 57.23°, and 62.84° for planes (220), (311), (400), (422), (511), and (440), respectively (Figure 2(c)). At 50 °C, there is instability in the XRD pattern and the appearance of impurity peaks was found at 70 °C. The reason is owing to the existence of intermediate product FeOOH. Higher temperature did not support the forming of Fe_3O_4 and as a result, the by-product was generated [28]. The characteristic peaks of Fe_3O_4 are all found at 30 °C and 90 °C. The formation of Fe_3O_4/thiamine at 30 °C indicates advantages such as a simple synthesis process and also protection of thiamine from chemical changes under high temperatures.

The effect of reaction time is revealed in Figure 2d at fixed reaction factors such as concentration of NH_4OH = 10%, mass ratio of $FeCl_2$:thiamine = 5:1 (g g^{-1}) and reaction temperature = 30 °C. The obtained results represent the characteristic peaks at 2θ = 29.97°, 35.26°, 42.98°, 53.32°, 57.06°, and 62.51° corresponding to planes (220), (311), (400), (422), (511), and (440), respectively. At 30 min, the XRD results show that its struction is almost amorphous because of the short reaction time, so the product was either not formed yet or too little was formed. With a prolonged reaction time from 60 to 120 min, the characteristic peaks of Fe_3O_4 were formed and gradually stabilized. The intensity of the diffraction peaks increases with increasing reaction time, while the peak width becomes narrower, indicating that the crystal size increases [10, 30]. Therefore, the synthesis time should be within 120 min.

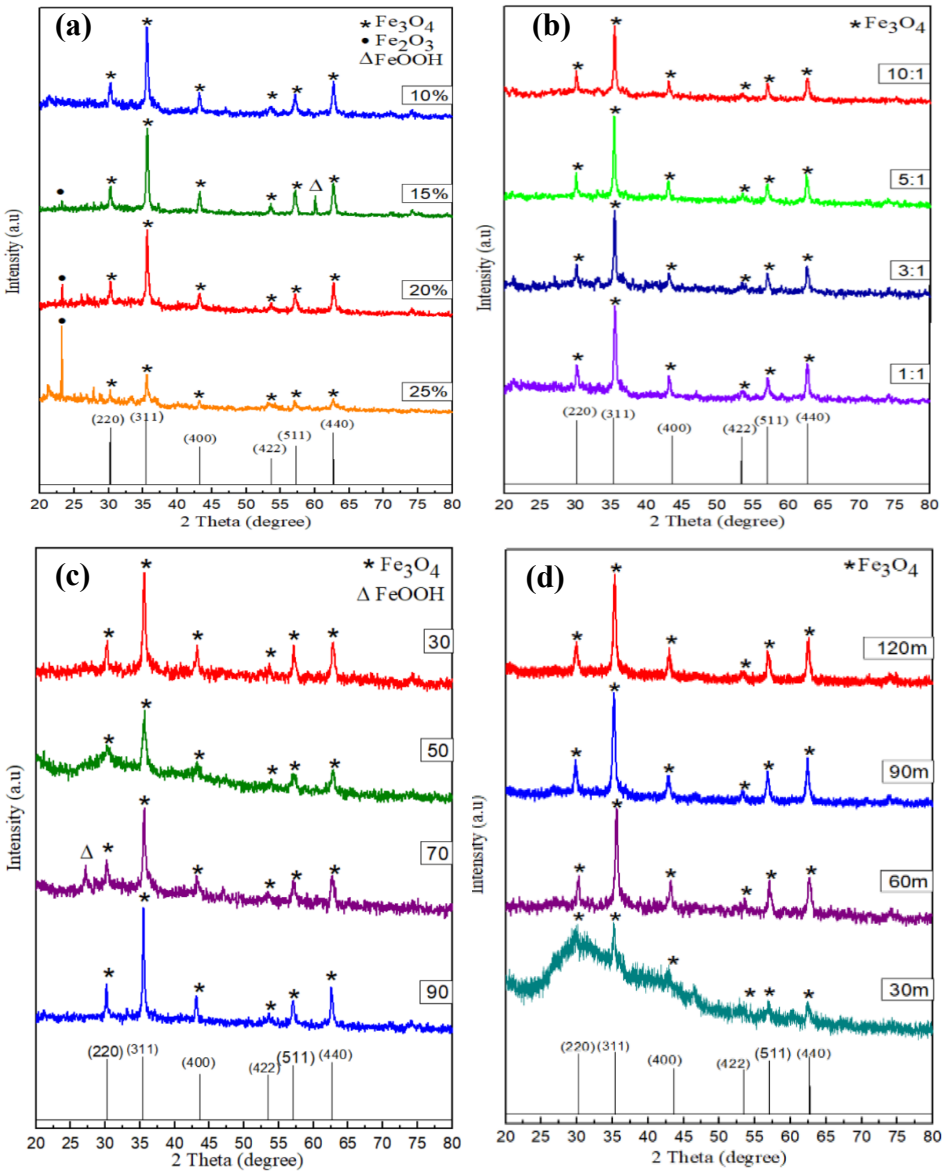

Figure 2 XRD patterns of Fe_3O_4/thiamine at (a) NH_4OH concentration of 10 – 25 %, (b) $FeCl_2.4H_2O$: thiamine = 1:1-10:1 (g g^{-1}), (c) 30 – 90 °C (c), and (d) 30 – 120 min.

Fe_3O_4/thiamine synthesized under the optimal conditions (NH_4OH concentration = 10%, mass ratio of $FeCl_2$:thiamine = 5:1 (g g^{-1}), reaction temperature = 30 °C, reaction time = 120 min) were selected for analyzing its chemo-physical properties. N_2 adsorption and desorption curves are class IV and have a 3-type hysteresis according to the International Union of Pure and Applied Chemistry (IUPAC) (Figure 3(a)) [31] and Fe_3O_4/thiamine is a mesoporous material following the isotherm curves. The pore size distribution curve of Fe_3O_4/thiamine is at about 200 E. Additionally, the specific surface area, pore diameter, and pore volume of Fe_3O_4/thiamine are determined based on the above analyses, namely 57.868 m^2 g^{-1}, 192.666 E, and 0.333 cm^3 g^{-1}, respectively. The magnetization of Fe_3O_4/thiamine at room temperature in Figure 3(b) exhibits paramagnetic properties and a saturation magnetization of about 2.4 emu g^{-1}. Fe_3O_4/thiamine was recovered under the influence of an external magnetic field, with the potential for easy retrieval after adsorption [32]. The DLS result reveals that the size of at most 50% of Fe_3O_4/thiamine is 300 nm, with 30% less than 300 nm, and 20% larger than 300 nm; with an average size of 293.7 nm in Figure 3(c).

Figure 4(a) presents the TEM results of Fe_3O_4/thiamine at different levels of 200 nm, 100 nm, and 50 nm. The material forms the core-shell structure of the thiamine-coated Fe_3O_4 nano-sheet with Fe_3O_4 possessing a polygonal shape and is relatively uniform. The particle size is about 50 nm, in the range of 40 to 60 nm. SEM images also had the similar morphology to TEM results and proving that Fe_3O_4/thiamine particles had the regular shape. The chemical composition of Fe_3O_4/thiamine was illustrated in Figure 4b, the weight percentage of Fe, O and C were 86.47%, 11.67% and 1.86%, respectively.

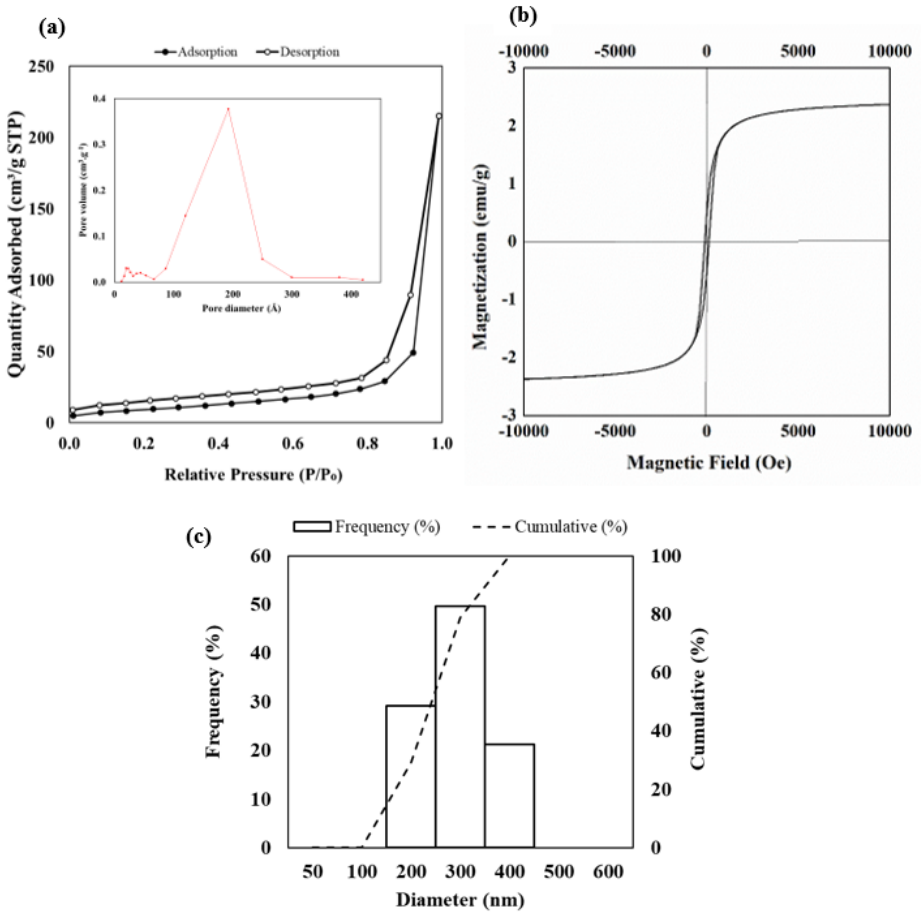

Figure 3 Plots showing (a) N_2 adsorption-desorption curves (pore size distribution curve– inset), (b) magnetization curve and (c) particle size distribution.

(a)

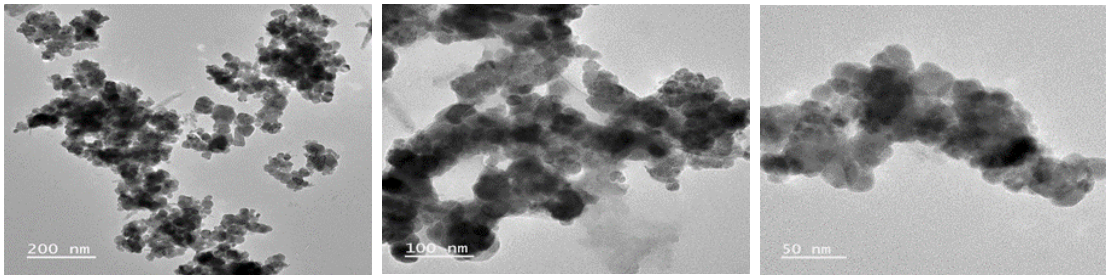

(b)

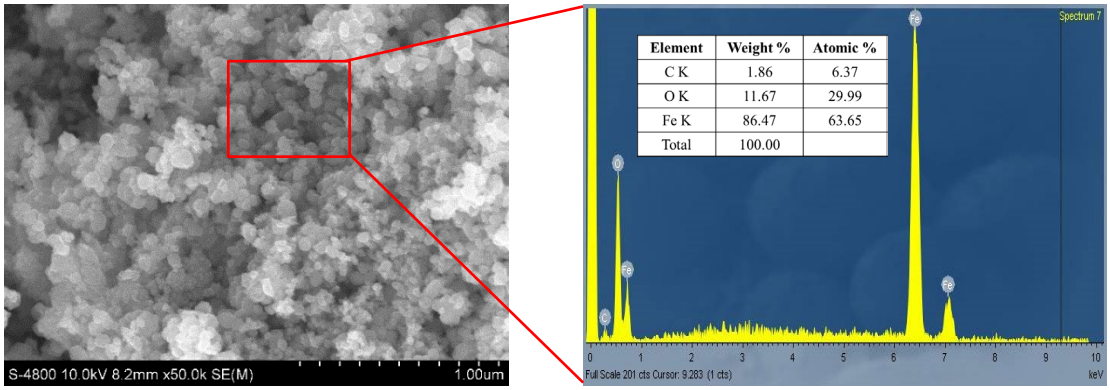

Figure 4 Pictures of (a) TEM images of Fe_3O_4/thiamine and (b) SEM images and EDX of Fe_3O_4/thiamine.

Synthesized Fe_3O_4 magnetic under various conditions are listed in Table 1. In this work, the base concentration (10%) used is lower than that of other studies. Using higher base concentration, the purification and washing steps will be more complicated and time-consuming. Thiamine reduces the possible oxidation of Fe_3O_4 at the mass ratio of 5:1, which corresponds to a molar ratio of 1:0.15 and is less than that of the studies of Shaterian [21] and Tran-Nguyen et al. [20]. Besides, the precipitation method used in this work helps saving the amount of inert gas. The reaction temperature (30 °C) is lower than that of most published studies, which makes the synthesis simple, easily implemented energy saving. Moreover, the time consumption of 120 min is also shorter than that of other studies. The surface area of Fe_3O_4/thiamine is 57 m^2 g^{-1}, which is higher than the other studies (about 35, 33, and 24 m^2 g^{-1}) [19–20, 33]. The presence of thiamine affects the surface area of Fe_3O_4.

2) MB adsorption by Fe_3O_4/thiamine

The isoelectric point of the synthesized Fe_3O_4/thiamine is 5.875 (data not shown); thus, pH value from 6–10 was selected. The pH of the solution was the main factor affecting the adsorption efficiency of MB dye [35]. Figure 5(a) reports that the adsorption efficiency and capacity increase with increasing pH value and it is consistent with the trend of surface charge. At pH 6 (near the isoelectric point), the adsorption efficiency was the lowest (43.805%). An increase in pH leads to a density increase in the adsorbent negative charge due to the binding of OH^- ions to the surface, so the adsorbent adsorbs more cationic dyes [35–36]. The surface of Fe_3O_4/thiamine is, then, negatively charged due to the excess of OH^- groups in the solution, leading to an interaction between the adsorbent and the positive amine groups of MB to form a stable bond between Fe_3O_4/thiamine and MB. The maximum yield and capacity are 78.285% and 6.263 mg g^{-1}, respectively at pH10. The adsorption happens by electrostatic attraction, which mainly depends on the pH of the solution and the point of zero charges (pH_{pzc}) [35–36]. MB is a cationic dye with a positive charge, otherwise, Fe_3O_4/thiamine has a negative charge. In case the pH of the solution is higher than pH_{pzc}, Fe_3O_4/thiamine attracts MB^+ ions, conducive to adsorption leading to the formation of MB- Fe_3O_4/thiamine magnetic complexes [2].

Table 1 Comparison of synthesized magnetic materials in this study and published works

Materials	Reaction conditions				S^b (m^2 g^{-1})	D^c (E)	Ref
	Base concentration	Molar ratio[a]	t (°C)	T (h)			
Fe_3O_4@thiamine	NH_4OH 25%	1:1	r.t.[d]	3	-	-	[21]
Fe_3O_4/PAA@SiO_2	NH_4OH 25%	-	200	12	163	-	[34]
Fe_3O_4-TiO_2	NH_4OH 28%	1:1	185	12	24.760	35.220	[33]
Thiamine modified-Fe_3O_4	NH_4OH	1:1	90	1	35.780	-	[20]
Fe_3O_4/thiamine	NH_4OH	-	90	2	32.999	329.130	[19]
Fe_3O_4/thiamine	NH_4OH 10%	1 : 0.15	30	2	57.870	192.670	This study

Remark: [a] the molar ratio of $FeCl_2$:thiamine; [b] specific surface area; [c] pore diameter; [d] room temperature

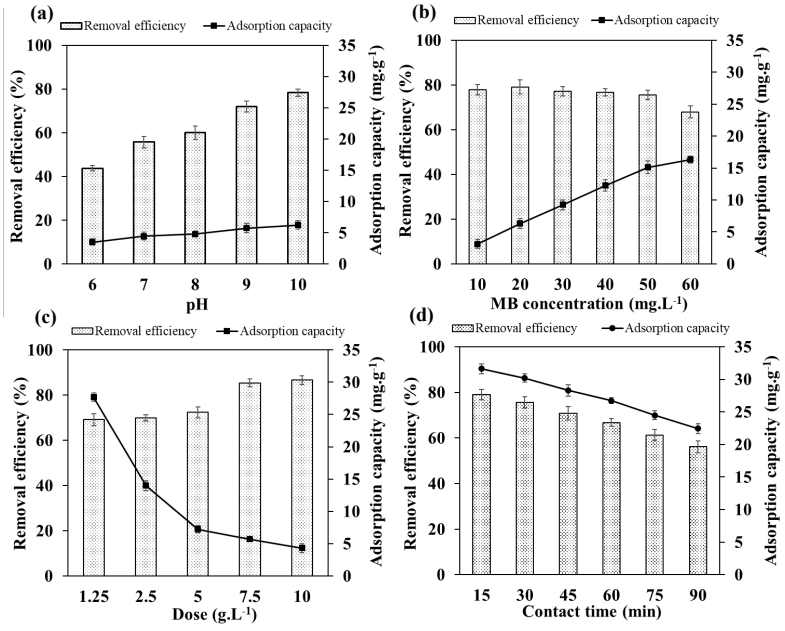

Figure 5 Plots showing effects of (a) pH (a), (b) MB concentration, (c) dose of Fe_3O_4/thiamine, and (d) contact time on the adsorption of MB.

Figure 5(b) reveals the effect of initial MB concentration (from 10 to 60 mg L^{-1}) on the removal efficiency and adsorption capacity. At the lowest MB concentration (10 mg L^{-1}), the adsorption efficiency and adsorption capacity are 77.889% and 3.116 mg g^{-1}, respectively. An increase of MB concentration between 10 and 50 mg L^{-1} did not change the removal efficiency because the adsorption process had reached the equilibrium, and the removal efficiency slightly reduced to 75% at 60 mg L^{-1} MB concentration. Besides, the adsorption capacity significantly increased about 5 times (between 3.116 mg g^{-1} and 16.315 mg g^{-1}) with an increase of MB concentration from 10 to 60 mg L^{-1}. The initial dye concentration was high, resulted in a decrease of dye removal rate, although the actual amount of dye adsorbed per unit mass increased [37]. The rise of initial dye concentration led to better dye adsorption capacity owing to more MB molecules as well as interactions increase between MB+ ion and the active sites of adsorbent [38]. A concentration of 50 mg L^{-1} (removal efficiency of 75.511%, adsorption capacity of 15.102 mg g^{-1}) was selected to conduct further experiments.

The influence of the Fe_3O_4/thiamine dosage (1.25 – 10 g L^{-1}) on MB adsorption is illustrated in Figure 5c. More adsorbent added resulted in higher efficiency (an increase of 17.44%, from 69.170% to 86.608%) whereas the adsorption capacity gradually dropped from 27.668 to 4.330 mg g^{-1} at the increase of dose between 1.25 and 10 g L^{-1}. The enhancement of dye removal efficiency could be due to increasing the surface area via adding more active sites [39]. An ideal adsorbent should be cost-effective and be able to adsorb a larger amount of dye ions from the solution at a smaller adsorbent dose [24]. A dose of Fe_3O_4/thiamine of 1.25 g L^{-1} was chosen with a removal efficiency of 69.168% and an adsorption capacity of 27.668 mg g^{-1}.

The contact time in Figure 5d is differed from 15 to 90 min to investigate the change in MB removal efficiency and adsorption capacity of Fe_3O_4/thiamine. At first 15 min, an efficiency of 79.078% indicates the rapid adsorption rate. A prolonged contact time resulted in a decrease of removal efficiency and adsorption capacity. The initial adsorption rate was fast because the dye ions were adsorbed by the external surface of adsorbent [37]. In the first stage, vacant sites on the surface of Fe_3O_4/thiamine were quickly filled, so extending contact time resulted in decreasing removal efficiency. This is attributed to the saturation of adsorption sites on the Fe_3O_4/thiamine surface; thus, the adsorbed dye ions tended to be released into the solution leading to lower adsorption efficiency and capacity [40]. A contact time of 15 min with the removal efficiency and adsorption capacity of 79.078% and 31.631 mg g^{-1}, respectively, was selected as the optimal time for MB adsorption.

3) Adsorption kinetic models

The pseudo-first-order and pseudo-second-order kinetics models were used to describe the adsorption rate and time for MB removal and adsorption mechanism between adsorbent and adsorbate. The plots that depict the calculated data according to the kinetic models are exhibited in Figure 6. The correlation coefficients of both models are quite high, namely 0.9679 for the pseudo-first-order and 0.9872 for the pseudo-second-order. The calculated adsorption capacities for the pseudo-first and second-order kinetic are 1.50 mg g^{-1} and 21.37 mg g^{-1}, respectively. The experimental capacity ($q_{e,exp}$ = 31.631 mg g^{-1}) and the calculated capacity ($q_{e,cal}$ = 21.37 mg g^{-1}) of the second-order kinetic are close (Table 2); hence, MB adsorption by Fe_3O_4/thiamine is described better by the second-order adsorption kinetics. This demonstrated that the adsorption process involves electrostatic interactions between the charge-rich N atom of MB and the Fe_3O_4/thiamine surface [22].

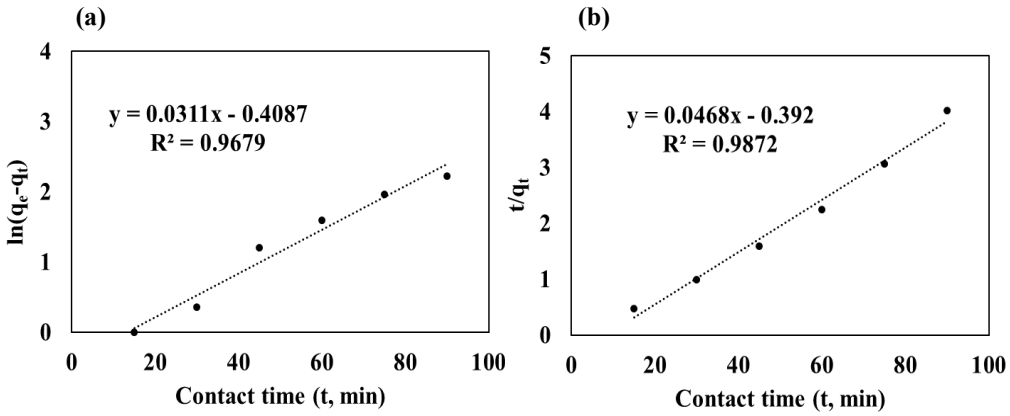

Figure 6 Plots of (a) pseudo-first-order and (b) pseudo-second-order models.

Table 2 Kinetic parameters for the adsorption of MB onto Fe_3O_4/thiamine

$q_{e,exp}$ (mg g^{-1})	Pseudo-first-order			Pseudo-second-order		
	$q_{e,cal}$ (mg.g^{-1})	K_1 (min^{-1})	R^2	$q_{e,cal}$ (mg g^{-1})	K_2 (g mg^{-1} min^{-1})	R^2
31.631	1.50	0.0311	0.9679	21.37	0.0059	0.9872

4) Adsorption isotherm models

Adsorption isotherm models were applied to investigate the MB adsorption of Fe_3O_4/thiamine. The correlation coefficients of the Langmuir and Freundlich models are 0.8475 and 0.9596, respectively (Figure 7(a) and Figure 7(b)). The Freundlich adsorption isotherm model is the preferred model. The adsorption process is reversible, the adsorption energy on the surface is not uniform, and there is an interaction between the adsorbed molecules [31, 41]. More than one layer of MB molecules may exist on the surface of Fe_3O_4/thiamine, resulting in the difficult contact between dye ions and adsorbent, and the adsorption process might be related to the agglomeration of dye molecules on surface [41]. According to the Dubinin – Radushkevich model in Figure 7(c), the average adsorption energy calculated is 0.52 kJ mol^{-1}, which is considerably less than 8 kJ mol^{-1}. Thus, MB adsorption by Fe_3O_4/thiamine is a physical adsorption process.

5) MB adsorption mechanism of Fe_3O_4/thiamine

The characteristic vibrations of Fe_3O_4/thiamine before and after MB adsorption are revealed in Figure 8(a). The strong absorption band at 586.11 cm^{-1} corresponds to the Fe-O bond [42]. The peaks of 2,890.03 cm^{-1}, 2,300.43 cm^{-1}, 1,512.23 cm^{-1}, 1,207.57 cm^{-1}, 1,023.32 cm^{-1}, and 751.19 cm^{-1} correspond to C-C, C-S, C=C, C-N, C-O, and C-S bonds, respectively; demonstrating the thiamine structure [21]. Fe_3O_4/thiamine has magnetic property and thiamine was not denatured during synthesis.

The change of surface functional groups of Fe_3O_4/thiamine after MB adsorption is depicted in Figure 8(b). The presence of MB is illustrated by peaks at 1,020.81, 1,353.01, 1,536.86 cm^{-1}, corresponding to CH_3–, C–N, C=S, respectively; hence, Fe_3O_4/thiamine after adsorption successfully carried MB molecules. Specifically, 1536.86 cm^{-1} peak is more sharpened, compared to that at 1512.23 cm^{-1} in Figure 8(a), and a significant increase in intensity may be ascribed to the attachment of MB on the surface of adsorbent [42]. Besides, functional groups at the surface of Fe_3O_4/thiamine are located as N-H (3,693.26 cm^{-1}), C-H (2,808.26 cm^{-1}), and C-O (1,020.81 cm^{-1}). The peak of C-O (1020.81 cm^{-1}) seems to be broadened and has a significant decrease in intensity, which may be ascribed to the electrostatic forces between the absorbent surface and MB [42]. Spectral analysis indicates that the driving force for the removal of MB using Fe_3O_4/thiamine is the electro-static attraction. As can be seen in Figure 7(c), there was no significant change between Fe_3O_4/thiamine before and after MB adsorption. Although the intensity of the peaks is decreased, the characteristic peaks are still preserved; this indicates that Fe_3O_4/thiamine retained its original crystal structure.

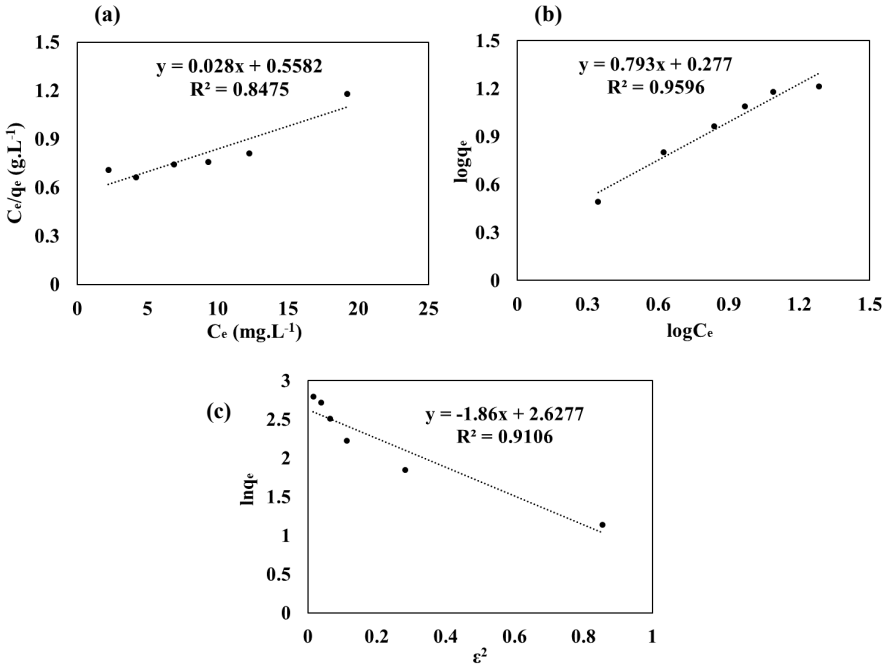

Figure 7 Plots of (a) Langmuir, (b)Freundlich, and (c) and Dubinin – Radushkevich models.

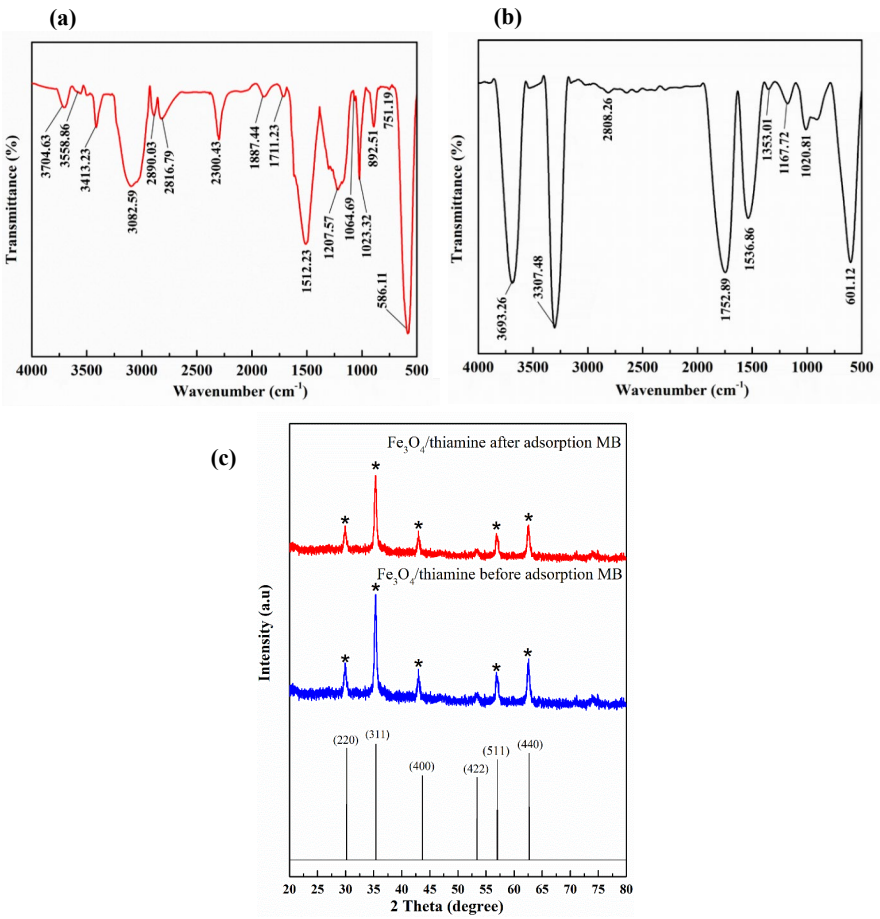

Figure 8 Pictures showing FTIR of Fe_3O_4/thiamine at the time of (a) before and (b) after MB adsorption and (c) XRD of Fe_3O_4/thiamine before and after MB adsorption.

The adsorption mechanism of MB onto Fe_3O_4/thiamine is mainly based on electrostatic interactions, hydrogen bonding and - interactions as described in Figure 9. The aromatic rings of thiamine could interact with the - bonds in the aromatic nucleus of MB [41]. Hydrogen bonding of Fe_3O_4/thiamine surface and the N atom of MB helped uptake dye ions onto Fe_3O_4/thiamine [43–44]. Additionally, the electrostatic interaction between the negative surface of Fe_3O_4/thiamine and the positive charge of MB also contributed importantly in the adsorption mechanism [43–45].

Adsorption capacity reported in some published works (Table 3) are considerably higher than that of this study. However, the adsorption capacity of this work is higher than that of HNT- Fe_3O_4 [46] and Fe_3O_4@SiO_2-CR [35]. Materials with different structures and under different adsorption conditions have different MB adsorption capacities. This creates a variety of treatment methods for organic dye in particular, and pollution problems in general.

6) Desorption

The reusability of Fe_3O_4/thiamine was explored by evaluating the change of adsorption efficiency after 3 reuse cycles (Figure 10). In this work, after MB adsorption, Fe_3O_4/thiamine attached MB was desorbed via 0.1 M HCl solution. Then, HCl solution containing MB was used for analyzing the MB concentration and the result exposed that 99.32% MB was removed from Fe_3O_4/thiamine indicating the desorption process was strongly occurred in acidic environment. Adsorption efficiency is 79.078% at the first use and remained fairly constant (78.563%) in the second reuse study. It dropped to 64.810% in the third cycle experiment. It can be suggested that Fe_3O_4/thiamine can be a potential and reusable adsorbent for treating MB in wastewater. This contributes to saving costs and resources, reducing environmental pollution.

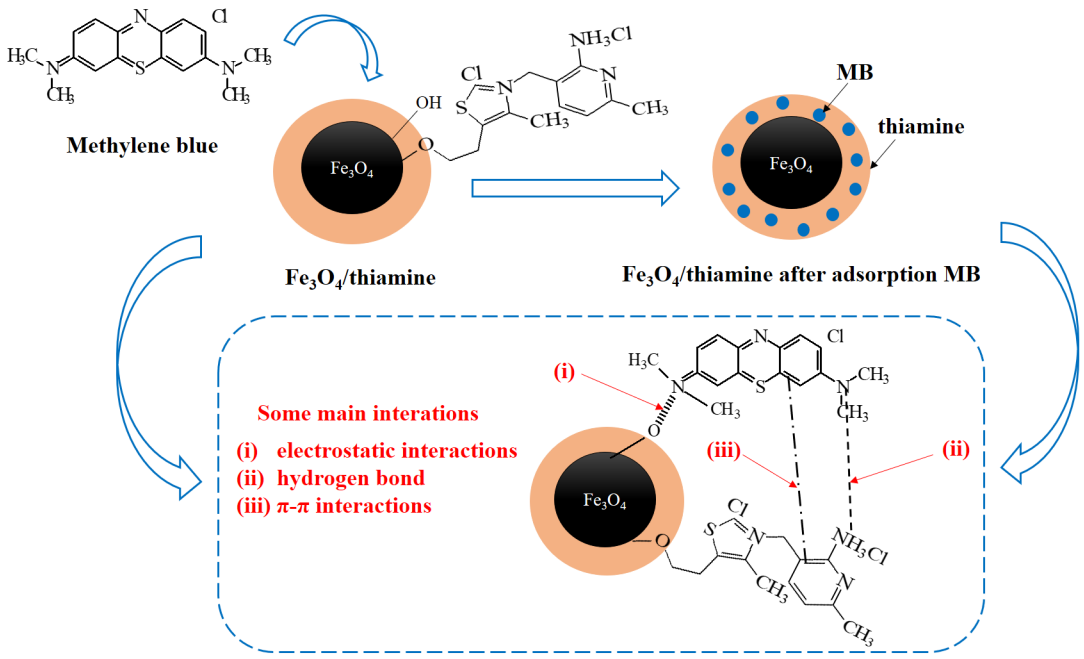

Figure 9 Proposed mechanism of MB adsorption onto Fe_3O_4/thiamine.

Table 3 Comparison of the MB adsorption of Fe_3O_4/thiamine and published works

Materials	Adsorption conditions		Adsorption capacity (mg g^{-1})	Ref
	pH	Time (min)		
Fe_3O_4/activated montmorillonite	7.37	25	47.96	[47]
Fe_3O_4@Ag/SiO_2	7	50	81.96	[39]
Fe_3O_4@SiO_2-CR	11	10	28.82	[35]
HNT-Fe_3O_4	-	480	18.49	[46]
Fe_3O_4/thiamine	10	15	31.63	This study

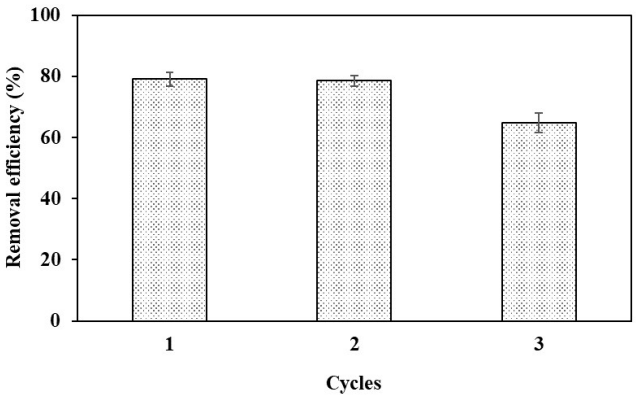

Figure 10 Removal efficiency of MB onto Fe_3O_4/thiamine in three adsorption-desorption cycles. Adsorption condition: 1.25 g L^{-1} of Fe_3O_4/thiamine, pH 10 in 15 min.

Conclusion

Fe_3O_4/thiamine was successfully synthesized with some advantages such as commercially available raw materials, and mild synthesis conditions without using inert gasses. Under optimal conditions including NH_4OH concentration = 10%, mass ratio of $FeCl_2$:thiamine = 5:1 (g g^{-1}), reaction temperature = 30 °C and reaction time = 120 min, XRD result shows that Fe_3O_4/thiamine has good crystallinity and less impurities. The specific surface area, pore diameter, and magnetization of Fe_3O_4/thiamine particles are 57.87 m^2 g^{-1}, 192.67 E, and 2.4 emu g^{-1}, respectively. Besides, the average particle size of Fe_3O_4/thiamine is approximately 293.7 nm. The core-shell structure of Fe_3O_4/thiamine is also depicted in the TEM images, with particles have a relatively uniform shape. The particle size is about 50 nm, in the range of 40 to 60 nm. The results of adsorption reveal that 79.08% of MB can be removed with a maximum adsorption capacity of 31.63 mg g^{-1} at pH 10, MB concentration of 50 mg L^{-1}, and contact time of 15 min. Adsorption kinetics studies exhibit that the experimental data are best fitted by the pseudo-second-order model. The physical adsorption process is appropriately described by the Freundlich isotherm adsorption model. After three cycles of adsorption-desorption, about 65% of adsorption efficiency remained, thus Fe_3O_4/thiamine can be a potential adsorbent for wastewater treatment.

References

[1] Zhang, X., Zhang, P., Wu, Z., Zhang, L., Zeng, G., Zhou, C. Adsorption of methylene blue onto humic acid-coated Fe_3O_4 nanoparticles. Colloids Surfaces A: Physicochemical Engineering Aspects, 2013, 435, 85–90.

[2] Pirbazari, A.E., Saberikhah, E., Kozani, S.H. Fe_3O_4–wheat straw: Preparation, characterization and its application for methylene blue adsorption. Water Resources Industry, 2014, 7, 23–37.

[3] Das, P., Nisa, S., Debnath, A., Saha, B. Enhanced adsorptive removal of toxic anionic dye by novel magnetic polymeric nanocomposite: optimization of process parameters. Journal of Dispersion Science and Technology, 2022, 43(6), 880–895.

[4] Deb, A., Debnath, A., Bhowmik, K., Rudra Paul, S., Saha, B. Application of polyaniline impregnated mixed phase Fe_2O_3, $MnFe_2O_4$ and ZrO_2 nanocomposite for rapid abatement of binary dyes from aqua matrix: response surface optimisation. International Journal of Environmental Analytical Chemistry, 2021, 1–19.

[5] Das, P., Debnath, A. Fabrication of $MgFe_2O_4$/polyaniline nanocomposite for amputation of methyl red dye from water: Isotherm modeling, kinetic and cost analysis. Journal of Dispersion Science and Technology, 2022, 1–12.

[6] Deb, A., Debnath, A., Saha, B. Sono-assisted enhanced adsorption of eriochrome Black-T dye onto a novel polymeric nanocomposite: Kinetic, isotherm, and response surface methodology optimization. Journal of Dispersion Science and Technology, 2021, 42(11), 1579–1592.

[7] Das, P., Debnath, A., Saha, B. Ultrasound-assisted enhanced and rapid uptake of anionic dyes from the binary system onto $MnFe_2O_4$/polyaniline nanocomposite at neutral pH. Applied Organometallic Chemistry, 2020, 34(8), e5711.

[8] Yari, M., Rajabi, M., Moradi, O., Yari, A., Asif, M., Agarwal, S., Gupta, V.K. Kinetics of the adsorption of Pb (II) ions from aqueous solutions by graphene oxide and thiol functionalized graphene oxide. Journal of Molecular Liquids, 2015, 209, 50–57.

[9] Chae, H.S., Kim, S.D., Piao, S.H., Choi, H.J. Core-shell structured Fe_3O_4@SiO_2 nanoparticles fabricated by sol–gel method and their magneto-rheology. Colloid Polymer Science, 2016, 294(4), 647–655.

[10] Vuong, T.K.O., Le, T.L., Pham, D.V., Pham, H.N., Le Ngo, T.H., Do, H.M., Nguyen, X.P. Synthesis of high-magnetization and monodisperse Fe_3O_4 nanoparticles via thermal decomposition. Materials Chemistry Physics, 2015, 163, 537–544.

[11] Liu, Y., Liu, P., Su, Z., Li, F., Wen, F. Attapulgite–Fe_3O_4 magnetic nanoparticles via co-precipitation technique. Applied Surface Science, 2008, 255(5), 2020–2025.

[12] Lu, T., Wang, J., Yin, J., Wang, A., Wang, X., Zhang, T. Surfactant effects on the microstructures of Fe_3O_4 nanoparticles synthesized by microemulsion method. Colloids Surfaces A: Physicochemical Engineering Aspects, 2013, 436, 675–683.

[13] Nabiyouni, G., Julaee, M., Ghanbari, D., Aliabadi, P.C., Safaie, N. Room temperature synthesis and magnetic property studies of Fe_3O_4 nanoparticles prepared by a simple precipitation method. Journal of Industrial Engineering Chemistry, 2015, 21, 599–603.

[14] Zhang, F., Zhao, Z., Tan, R., Guo, Y., Cao, L., Chen, L., ..., Song, W. Selective and effective adsorption of methyl blue by barium phosphate nano-flake. Journal of Colloid Interface Science, 2012, 386(1), 277–284.

[15] Yu, S., Wang, J., Cui, J. Preparation of a novel chitosan-based magnetic adsorbent CTS@SnO_2@Fe_3O_4 for effective treatment of dye wastewater. International Journal of Biological Macromolecules, 2020, 156, 1474–1482.

[16] Aslam, S., Zeng, J., Subhan, F., Li, M., Lyu, F., Li, Y., Yan, Z. In situ one-step synthesis of Fe_3O_4@MIL-100 (Fe) core-shells for adsorption of methylene blue from water. Journal of Colloid Interface Science, 2017, 505, 186–195.

[17] Mallakpour, S., Nouruzi, N. Application of vitamin B1-coated carbon nanotubes for the production of starch nanocomposites with enhanced structural, optical, thermal and Cd (II) adsorption properties. Journal of Polymers, 2018, 26(7), 2954–2963.

[18] Liang, W., Hu, H.Y, Song, Y.D., Wang, H., Guo, Y.F. Effects of thiamine on treatment performance of textile wastewater. Desalination, 2009, 242(1–3), 110–114.

[19] Angkawijaya, A.E., Tran-Chuong, Y.N., Ha, Q.N, Tran-Nguyen, P.L., Santoso, S.P., Bundjaja, V., …, Ju, Y.H. Studies on the performance of functionalized Fe_3O_4 as phosphate adsorbent and assessment to its environmental compatibility. Journal of the Taiwan Institute of Chemical Engineers, 2022, 131, 104162.

[20] Tran-Nguyen, P.L., Angkawijaya, A.E., Ha, Q.N., Tran-Chuong, Y.N., Go, A.W., Bundjaja, V., …,

Ju, Y.H. Facile synthesis of superparamagnetic thiamine/Fe_3O_4 with enhanced adsorptivity toward divalent copper ions. Chemosphere, 2022, 291, 132759.

[21] Shaterian, H.R., Molaei, P. Fe_3O_4@vitamin B1 as a sustainable superparamagnetic heterogeneous nanocatalyst promoting green synthesis of trisubstituted 1, 3-thiazole derivatives. Applied Organometallic Chemistry, 2019, 33(7), e4964.

[22] Singh, N.J., Wareppam, B., Kumar, A., Singh, K.P., Garg, V.K., Oliveira, A.C., Singh, L.H. Zeolite incorporated iron oxide nanoparticle composites for enhanced Congo red dye removal. Journal of Materials Research, 2023, 38(4), 1149–1161.

[23] Rezaei, H., Haghshenasfard, M., Moheb, A. Optimization of dye adsorption using Fe_3O_4 nanoparticles encapsulated with alginate beads by Taguchi method. Adsorption Science & Technology, 2017, 35(1–2), 55–71.

[24] Mittal, H., Ballav, N., Mishra, S.B. Gum ghatti and Fe_3O_4 magnetic nanoparticles based nanocomposites for the effective adsorption of methylene blue from aqueous solution. Journal of Industrial Engineering Chemistry, 2014, 20(4), 2184–2192.

[25] Yuanbi, Z., Zumin, Q., Huang, J. Preparation and analysis of Fe_3O_4 magnetic nanoparticles used as targeted-drug carriers. Chinese Journal of Chemical Engineering, 2008, 16(3), 451–455.

[26] Jia, B., Gao, L. Fabrication of Fe_3O_4 core-shell polyhedron based on a mechanism analogue to Ostwald ripening process. Journal of Crystal Growth, 2007, 303(2), 616–621.

[27] Zaitsev, V.S., Filimonov, D.S., Presnyakov, I.A., Gambino, R.J., Chu, B. Physical and chemical properties of magnetite and magnetite-polymer nanoparticles and their colloidal dispersions. Journal of Colloid Interface Science, 1999, 212(1), 49–57.

[28] Yan, H., Zhang, J., You, C., Song, Z., Yu, B., Shen, Y. Influences of different synthesis conditions on properties of Fe_3O_4 nanoparticles. Materials Chemistry Physics, 2009, 113(1), 46–52.

[29] Zhang, H., He, X., Zhao, W., Peng, Y., Sun, D., Li, H., Wang, X. Preparation of Fe_3O_4/TiO_2 magnetic mesoporous composites for photocatalytic degradation of organic pollutants. Water Science Technology, 2017, 75(7), 1523–1528.

[30] Rafiee, F., Mehdizadeh, N. Palladium n-heterocyclic carbene complex of vitamin B1 supported on silica-coated Fe_3O_4 nanoparticles: A green and efficient catalyst for C–C coupling. Catalysis Letters, 2018, 148(5), 1345–1354.

[31] Qi, L., Jiaqi, Z., Yimin, D., Danyang, L., Shengyun, W., Ling, C. Facile synthesis of 5-aminoisophthalic acid functionalized magnetic nanoparticle for the removal of methylene blue. Journal of Materials Science: Materials in Electronics, 2020, 31, 457–468.

[32] Bao, X., Qiang, Z., Chang, J.H., Ben, W., Qu, J. Synthesis of carbon-coated magnetic nanocomposite (Fe_3O_4@C) and its application for sulfonamide antibiotics removal from water. Journal of Environmental Sciences, 2014, 26(5), 962–969.

[33] Zazouli, M.A., Ghanbari, F., Yousefi, M., Madihi-Bidgoli, S. Photocatalytic degradation of food dye by Fe_3O_4–TiO_2 nanoparticles in presence of peroxymonosulfate: The effect of UV sources. Journal of Environmental Chemical Engineering, 2017, 5(3), 2459–2468.

[34] Xuan, S., Wang, F., Lai, J.M., Sham, K.W., Wang, Y.X.J., Lee, S.F., …, Leung, K.C.F. Synthesis of biocompatible, mesoporous Fe_3O_4 nano/ microspheres with large surface area for magnetic resonance imaging and therapeutic applications. ACS Applied Materials & Interfaces, 2011, 3(2), 237–244.

[35] Yimin, D., Jiaqi, Z., Danyang, L., Lanli, N., Liling, Z., Yi, Z., Xiaohong, Z. Preparation of Congo red functionalized Fe_3O_4@SiO_2 nanoparticle and its application for the removal of methylene blue. Colloids Surfaces A: Physicochemical Engineering Aspects, 2018, 550, 90–98.

[36] Zhang, Z., Zhao, X., Jv, X., Lu, H., Zhu, L. A simplified method for synthesis of l-tyrosine modified magnetite nanoparticles and its application for the removal of organic dyes. Journal of Chemical Engineering Data, 2017, 62(12), 4279–4287.

[37] Ghaedi, M., Hassanzadeh, A., Kokhdan, S.N. Multiwalled carbon nanotubes as adsorbents for the kinetic and equilibrium study of the removal of Alizarin Red S and Morin. Journal of Chemical Engineering Data, 2011, 56(5), 2511–2520.

[38] Song, N., Wu, X.L., Zhong, S., Lin, H., Chen, J.R. Biocompatible G-Fe_3O_4/CA nanocomposites for the removal of methylene blue. Journal of Molecular Liquids, 2015, 212, 63–69.

[39] Saini, J., Garg, V., Gupta, R. Removal of methylene blue from aqueous solution by Fe_3O_4@Ag/SiO_2 nanospheres: Synthesis, characterization and adsorption performance. Journal of Molecular Liquids, 2018, 250, 413–422.

[40] Kurniawati, D., Sari, T.K., Adella, F., Sy, S. Effect of contact time adsorption of Rhodamine B, Methyl Orange and Methylene blue colours on Langsat shell with batch methods. Journal of Physics: Conference Series, IOP Publishing, 2021, 1788(1), 012008.

[41] Ma, J., Yu, F., Zhou, L., Jin, L., Yang, M., Luan, J., …, Chen, J. Enhanced adsorptive removal of methyl orange and methylene blue from aqueous solution by alkali-activated multiwalled carbon nanotubes. ACS Applied Materials & Interfaces, 2012, 4(11), 5749–5760.

[42] Li, W., Zhang, B., Li, X., Zhang, H., Zhang, Q. Preparation and characterization of novel immobilized Fe_3O_4@SiO_2@mSiO_2–Pd (0) catalyst with large pore-size mesoporous for Suzuki coupling reaction. Applied Catalysis A: General, 2013, 459, 65–72.

[43] Zhang, P., O'Connor, D., Wang, Y., Jiang, L., Xia, T., Wang, L., …, Houa, D. A green biochar/iron oxide composite for methylene blue removal. Journal of Hazardous Materials, 2020, 384, 121286.

[44] Nasar, A., Mashkoor, F. Application of polyaniline-based adsorbents for dye removal from water and wastewater—A review. Environmental Science and Pollution Research, 2019, 26, 5333–5356.

[45] Sakthivel, S., Periakaruppan, R., Vallinayagam, S., Gandhi, S., Tappa, M.M., Sharma, V.K., …, Gurusamy, A. Synthesis and characterization of paddy straw chitosan nanocomposite as an efficient photocatalytic bio-adsorbent for the removal of Rhodamine B and Malachite green dye from aqueous solution. Applied Nanoscience, 2023, 13(3), 2555–2569.

[46] Xie, Y., Qian, D., Wu, D., Ma, X. Magnetic halloysite nanotubes/iron oxide composites for the adsorption of dyes. Chemical Engineering Journal, 2011, 168(2), 959–963.

[47] Chang, J., Ma, J., Ma, Q., Zhang, D., Qiao, N., Hu, M., Ma, H., Adsorption of methylene blue onto Fe_3O_4/activated montmorillonite nanocomposite. Applied Clay Science, 2016, 119, 132–140.